Available online at www.sciencedirect.com

SCIENCE DIRECT®

Catalysis Today 113 (2006) 215–219

CATALYSIS TODAY

www.elsevier.com/locate/cattod

ZnTe precipitates formed in SiO_2 by sequential implantation of Zn^+ and Te^+ ions

R. Chemam [a,b,*], J.J. Grob [b], A. Bouabellou [c], D. Muller [b]

[a] *Laboratoire LPR, Département de Physique, Faculté des Sciences, Université de Annaba, BP 12 Annaba, 23000 Algérie, France*
[b] *Laboratoire PHASE (UPR 292 du CNRS), 23, rue du Loess, 67037 Strasbourg Cedex 2, France*
[c] *Laboratoire Couches Minces et Interfaces, Université Mentouri de Constantine, Constantine 25000, Algérie, France*

Abstract

Ion implantation is a versatile tool for the formation of compound semiconductor nanocrystal precipitates in a host medium with the ultimate goal to form quantum dots for use in device technology. Low dose (1×10^{16} cm^{-2}) implantations of tellurium and zinc ions have been performed in a 250 nm thick SiO_2 layer thermally grown on ⟨1 1 1⟩ silicon. Their respective energies (180 and 115 keV) have been chosen to produce 5–10 at.% profiles overlapping at a mean depth of about 100 nm. Subsequent thermal treatments at 700 and 800 °C lead to the formation of nanometric precipitates of the compound semiconductor ZnTe. Their size, crystalline structure and depth distribution have been studied as a function of annealing temperature using transmission electron microscopy (TEM) and Rutherford backscattering spectrometry. For the lowest temperature the TEM images shows a cloudy band of ZnTe, but for the highest temperature, the ZnTe nanocrystals are self organized into two layers parallel to the surface. Their mean diameter ranges between 4 and 30 nm, as a function of annealing temperature.

PACS: 61.72.−y; 85.40.Ry; 81.40.Ef; 81.07.Bc; 61.72.Dd

Keywords: Ion implantation; Nanoparticles; Heat treatment; Self-organization; ZnTe; Si; SiO_2

1. Introduction

In the past few years, an intense research activity was devoted to develop technology for the efficient and well reproducible synthesis of nanocrystals (NCs) in various matrixes [1–7]. Control over the particle size allows strong modifications of electronic, optical and other properties of NCs, offering a number of potential applications in semiconductor device technology and other industries [1].

The main interest in direct band gap semiconductor NCs comes out from the pronounced effects of quantum confinement, strongly dependent on the particle size, which makes possible the tunability of the luminescence [8–12]. ZnTe is a II–VI compound semiconductor with a direct band gap of 2.25 eV at room temperature and exciton radius around 5 nm. This material has potential applications for a variety of optoelectronic devices such as pure green light-emitting diodes, solar cells, wave guides and modulators.

Using ion implantation, the NCs can be formed into the near-surface region of an appropriate host material. The nucleation and growth of the NCs are controlled mainly by subsequent annealing procedure and only in less extent by implantation parameters. There is a wide variety of NCs accessible by ion implantation, ranging from metallic NCs, single component semiconductors like Si and Ge, to compound semiconductors and alloys in different host materials (e.g. Si, $A1_2O_3$, Si_3N_4, SiO_2) [13–15]. Furthermore, this technique has the unique advantage to be fully compatible with the current semiconductor technology. Sequential implantation of equal doses of constituent atoms offers a simple way to produce nanocrystals of compound semiconductors [1,3,4,16,17]. The introduction of elements by ion implantation into a thin layer is also a great challenge since atomic transport is influenced by the interfaces which settle the boundary conditions. This work aims to verify whether a nanometric size can be obtained by implantation. More precisely, in this work, we look for optimum conditions (implantation dose, annealing temperature) to control size and/

---

* Corresponding author. Fax: +33 3 88 10 65 48.
E-mail address: che_raf@yahoo.fr (R. Chemam).

0920-5861/$ – see front matter © 2005 Elsevier B.V. All rights reserved.
doi:10.1016/j.cattod.2005.11.085

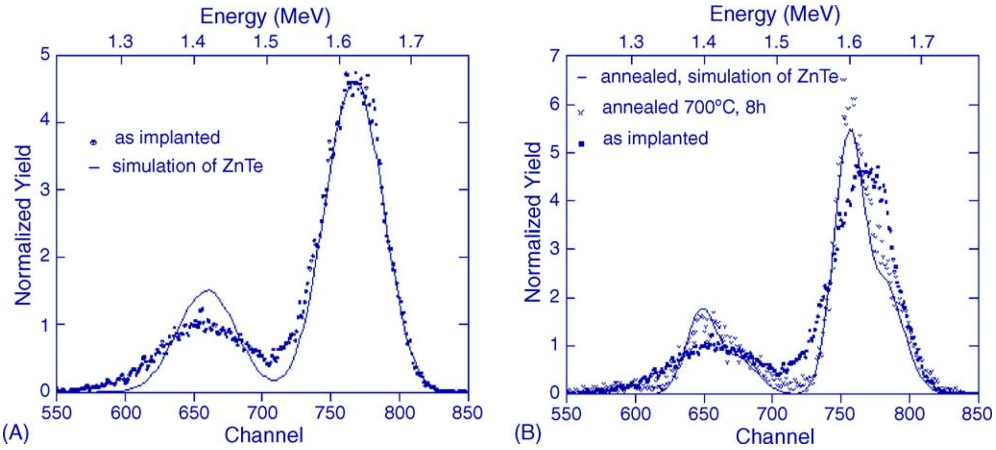

Fig. 1. RBS spectra of a SiO_2 sample implanted with Zn (115 keV) and Te (180 keV) at a dose of 1×10^{16} ion/cm^2: (A) as implanted and (B) annealed at 700 °C for 8 h (crosses).

or location of ZnTe particles formed by the successive implantation of Zn and Te in a thermally grown SiO_2 layer on silicon.

2. Experimental procedure

Substrates used in this work were 250 nm thick thermally grown SiO_2 layers on n-type ⟨1 1 1⟩ silicon wafers. Te^+ and Zn^+ ions were implanted using doses of 1×10^{16} ions/cm^2. Ion energies were selected using the SRIM 2000 [18] code so as to give overlapping concentration profiles and equal doses were used to reach the proper stoichiometry, accounting for profile modifications due to surface sputtering. For that, experimental values of bulk and surface binding energies have been used as SRIM input parameters [19]. Zinc was implanted first at 115 keV and then tellurium at 180 keV, resulting, according to the simulations, in a 5–10 at.% maximum concentration for each species, overlapping at about 100 nm in the oxide.

After implantation the samples are annealed at 700 and 800 °C under flowing nitrogen in a conventional furnace for times varying from 15 min to 2 h. The depth profiles of each element were measured by Rutherford backscattering spectroscopy (RBS). Two mega-electron volts He^+ particles at normal incidence and a scattering angle of 160° were used for most analysis, but in some cases, the depth resolution was improved using a glancing angle geometry. The RUMP program was used to simulate the RBS spectra [20].

Cross-sectional samples were prepared for transmission electron microscopy (TEM) analysis by gluing the implanted face to a Si wafer and hand-polishing to a thickness of 1 μm, as estimated by the color of the Si in transmitted light [21]. The specimens were then attached to a copper grid. TEM analysis was performed using a TOPCON 002B electron microscope operated at 200 kV. This apparatus is equipped with a Si(Li) detector, allowing a rough estimate of the chemical composition of the target, from the electron beam induced X-ray emission. From the RBS spectra, information on the concentration depth distribution were extracted and compared with the corresponding TEM images and X-ray fluorescence.

3. Results and discussion

Fig. 1A and B shows the RBS spectra of the as implanted sample (A) and that annealed at 700 °C for 8 h (B). The Zn and

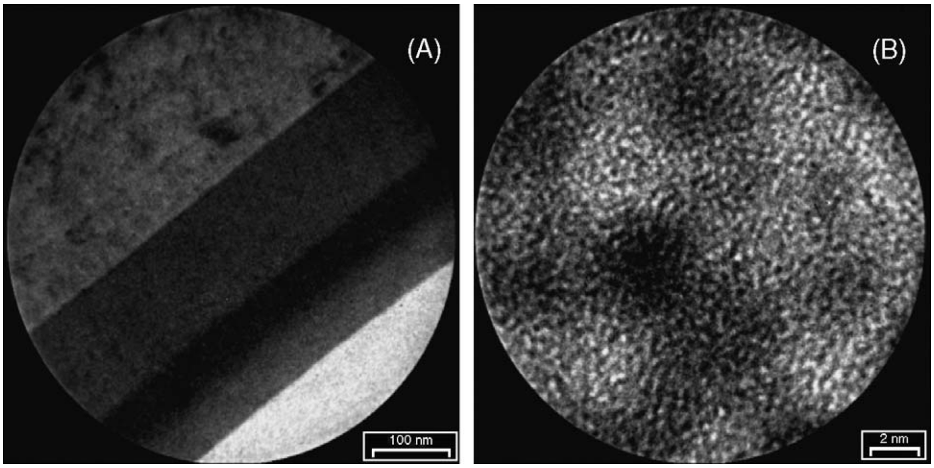

Fig. 2. TEM images of a sample implanted with Zn (115 keV) and Te (180 keV) ions at a dose of 1×10^{16} ion/cm^2 and annealed at 700 °C, 2 h: (A) general view of the SiO_2 layer and (B) high-resolution image of the implanted region.

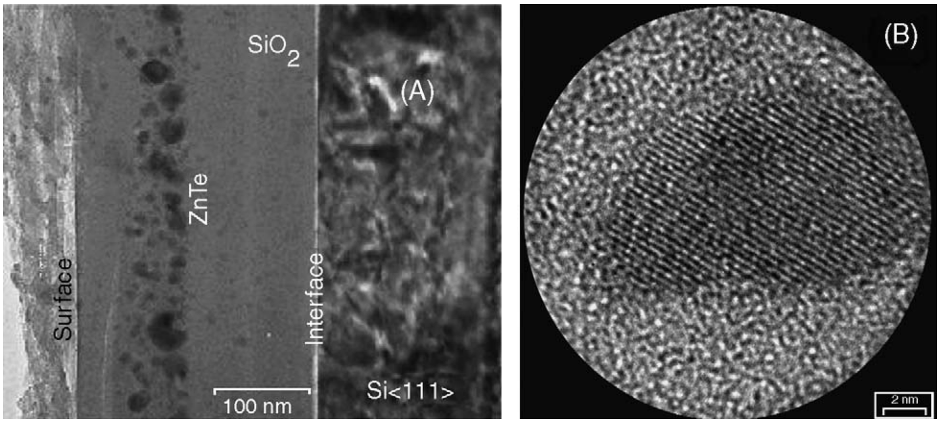

Fig. 3. TEM images of a sample implanted with Zn (115 keV) and Te (180 keV) ions at a dose of 1 × 10^{16} ion/cm^2 and annealed at 700 °C, 8 h: (A) general view of the SiO_2 layer and (B) high-resolution image of the implanted region.

Te distributions are well separated due to the large difference between their atomic masses. The depth resolution is enhanced using a 40° incidence angle and a 60° backward direction, relative to the sample normal. The RUMP simulations fitted to the experimental spectra show almost Gaussian-like concentration profiles. In the as-implanted state (Fig. 1A), the simulation shows that the two distributions are located roughly at the same depth (90 nm) and that there is a significant Zn deficiency at this depth, compared to the simulated equal concentration of each element. This is mainly due to the spreading of atoms during implantation, more pronounced for Zn than for Te. After annealing, Zn and Te precipitation or chemical reaction between the two elements can occur [5]. We observe (Fig. 1B) the shift and the narrowing of the distributions and the adjustment of the height of both Zn and Te signals to the level corresponding to the formation of the stoichiometric compound ZnTe. This suggests a redistribution of the species and that the chemical reaction actually happened. However, there is no evidence that the reaction is complete and/or there is no precipitation of the elements. So, as an attempt to clarify the situation, we have used the TEM technique.

The high-resolution TEM images in Fig. 2 correspond to the sample annealed at 700 °C for 2 h. Fig. 2A shows a 60 nm wide cloudy band in the SiO_2 layer located around 100 nm in depth. This band reflects the simple presence of Zn and Te atoms. An enlargement (Fig. 2B) of this cloud reveals nanometric black spots but it is difficult to conclude to the formation of nanocrystalline ZnTe compound. However, after 8 h annealing (Fig. 3A), the fuzzy band of Fig. 2 transforms into well separated precipitates, more or less organized in two bands. The high-resolution images of these clusters (Fig. 3B) show they are monocrystalline (or sometimes polycrystalline).

Fig. 4 illustrates RBS spectra of a sample annealed at 800 °C for 2 h. The RBS signals of Zn and Te this time clearly split in two peaks, indicating that a redistribution of the atomic species took place. This finding is confirmed by the cross-sectional TEM images, which are shown in Fig. 5 (15 min annealing) and

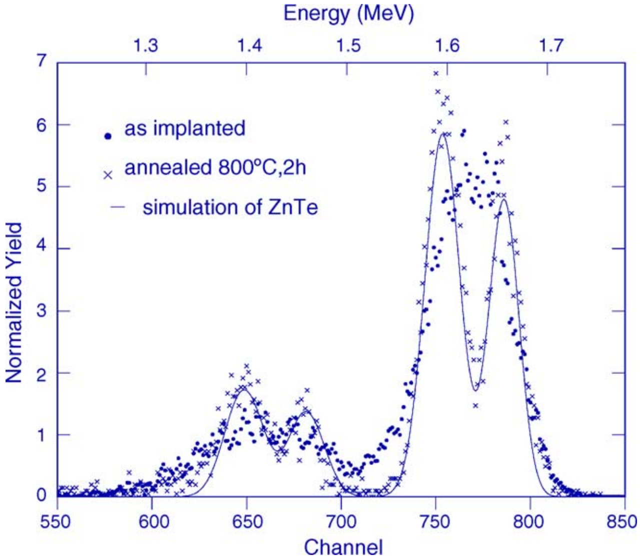

Fig. 4. RBS spectra of a SiO_2 sample implanted with Zn^+ (115 keV) and Te^+ (180 keV) at a dose of 1 × 10^{16} ion/cm^2: as implanted (black circles) and annealed at 800 °C for 2 h (crosses).

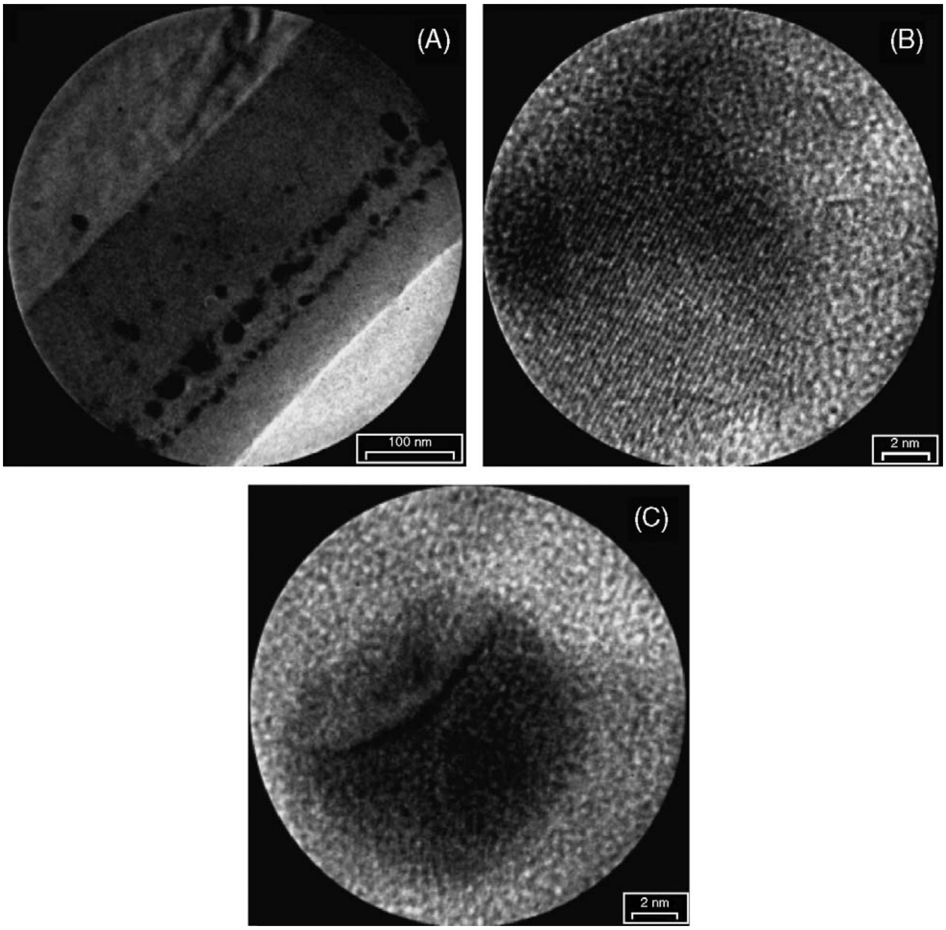

Fig. 5. TEM images of a sample implanted with Zn (115 keV) and Te (180 keV) ions at a dose of 1×10^{16} ion/cm^2 and annealed at 800 °C, 15 min: (A) general view of the SiO_2 layer, (B) high-resolution image of the implanted region and (C) high-resolution image shows extended crystalline defects.

Fig. 6 (2 h annealing). Both measurements lead to the conclusion that there are two well-separated bands of NCs formed after annealing in pure N_2 atmosphere. The first band of particles is located at 75 nm below the surface of the SiO_2 layer with an average width between 4 and 10 nm. The second band spreads over 20–30 nm at a depth of about 110 nm with NCs significantly greater than in the first band. Previous calculations of Reiss and Heinig [22] predict this phenomenon, which seems to be an intrinsic self-organization effect of NCs by the Ostwald ripening mechanism in inhomogeneous systems [23,24]. There is no spectacular evolution of these two bands with annealing time, except the spreading of the second band corresponding

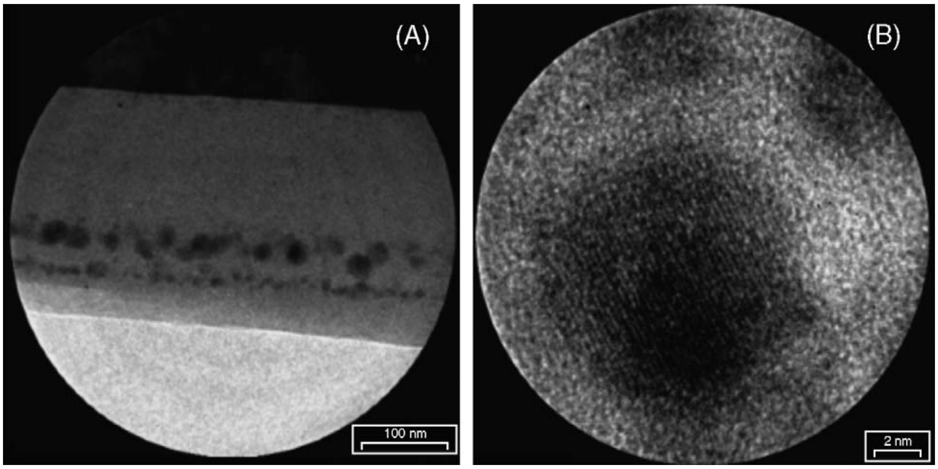

Fig. 6. TEM images of a sample implanted with Zn (115 keV) and Te (180 keV) ions at a dose of 1×10^{16} ion/cm^2 and annealed at 800 °C, 2 h: (A) general view of the SiO_2 layer and (B) high-resolution image of the implanted region.

to the coarsening (by migration and coalescence) of the nanoprecipitates.

High-resolution images of NCs in 15 min annealed samples (Fig. 5C) often reveal the presence of extended crystalline defects (grain boundary, low angle boundary and/or stacking faults). The crystalline quality seems to be better after 2 h annealing (Fig. 6B).

The energy-dispersive X-ray (EDX) microanalyses of these NCs during their high-resolution TEM observations, though not very accurate (since the beam probes also these parts of the matrix situated above and under the NC) gives results of the relative Zn and Te concentrations in reasonably good agreement with the stoichiometric ratio.

4. Conclusion

The formation of ZnTe NCs in thermally grown 250 nm thick SiO_2 on Si⟨1 1 1⟩ was achieved by sequential ion implantation of the Zn and Te elements at a dose of 1×10^{16} and subsequent annealing treatments. The resulting depth distributions of the NCs were investigated using RBS, TEM and X-ray fluorescence. At 700 °C, we have found that the profiles remain nearly unchanged, though the compound is formed. For the samples annealed at 800 °C, the RBS spectra show that both the Zn and Te signals split in two peaks. The corresponding TEM images confirm this result and show that there are two bands of NCs formed in the SiO_2 layer. The first layer is located at 75 nm below the surface with an average width between 4 and 10 nm; the second band is deeper, at about 110 nm with an average width between 20 and 30 nm. The mean diameter of the NCs in the second band is about 24 nm, significantly larger than in the first layer (8 nm). This self-organization into two layers can be explained by the Ostwald ripening process in inhomogeneous systems.

Acknowledgements

The authors wish to acknowledge Yann Le Gall who performed the implantation, Marianne Amann for her help to prepare the samples and Sebastien Joulie who performed the observations by electron microscopy.

References

[1] A. Meldrum, R.F. Haglund Jr., L.A. Boatner, C.W. White, Adv. Mater. 13 (2001) 1431.
[2] J.D. Budai, C.W. White, S.P. Wiothrow, M.F. Chisholm, J. Zhu, R.A. Zuhr, Nature 390 (1997) 384.
[3] C.W. White, A. Meldrum, J.D. Budai, S.P. Withrow, E. Sonder, R.A. Zuhr, D.M. Hembree Jr., M. Wu, D.O. Henderson, Nucl. Instrum. Meth. B 148 (1999) 991.
[4] H. Karl, I. Grosshans, W. Attenberger, M. Schmid, B. Stritzker, Nucl. Instrum. Meth. B 178 (2001) 126.
[5] I. Großhans, H. Karl, B. Stritzker, Nucl. Instrum. Meth. Phys. Res. B 190 (2002) 865.
[6] R. Chemam, A. Bouabellou, J.J. Grob, D. Muller, G. Schmerber, Nucl. Instrum. Meth. B 216 (2004) 116.
[7] U.V. Desnica, M. Buljan, I.D. Desnica-Frankovic, P. Dubcek, S. Bernstorff, M. Ivanda, H. Zorc, Nucl. Instrum. Meth. B 216 (2004) 407.
[8] D. Nesheva, Z. Levi, Z. Aneva, V. Nikolova, H. Hofmeister, J. Phys. Condens. Matter 12 (2000) 751.
[9] O. Wind, Dissertation, Universität Karlsruhe, 1997.
[10] A.L. Rogach, A. Eychmuller, J. Rockenberger, A. Kornowski, H. Weller, L. Troger, M.Y. Gao, M.T. Harrison, S.V. Kershaw, M.G. Burt, Mater. Res. Soc. Symp. Proc. 536 (1999) 365.
[11] C.W. White, J.D. Budai, S.P. Withrow, J.G. Zhu, E. Sonder, R.A. Zuhr, A. Meldrum, D.M. Hembree, D.O. Henderson, S. Prawer, Nucl. Instrum. Meth. B 141 (1998) 228.
[12] P. Lefebvre, H. Mathieu, J. Allegre, T. Richard, A. Combettes-Roos, M. Pauthe, W. Granier, Sci. Technol. 12 (1997) 958.
[13] A. Meldrum, C.W. White, L.A. Boatner, I.M. Anderson, R.A. Zuhr, E. Sonder, J.D. Budai, D.O. Henderson, Nucl. Instrum. Meth. B 148 (1999) 957.
[14] C.W. White, J.D. Budai, A.L. Meldrum, S.P. Withrow, R.A. Zuhr, E. Sonder, A. Purezky, D.B. Geohegan, J.G. Zhu, D.O. Henderson, Mater. Res. Soc. Proc. 504 (1998) 399.
[15] A. Meldrum, L.A. Boatner, C.W. White, Nucl. Instrum. Meth. B 178 (2001) 7.
[16] U.V. Desnica, I.D. Desnica-Frankovic, O. Gamulin, C.W. White, E. Sonder, R.A. Zuhr, J. Non-Cryst. Solids 299–302 (2002) 1100.
[17] U.V. Desnica, P. Dubcek, I.D. Desnica-Frankovic, M. Buljan, S. Bernstorff, S.W. White, J. Appl. Cryst. 36 (2003) 443.
[18] J.F. Ziegler, J.P. Biersack, U. Littmark, The Stopping and Range of Ions in Solids, Pergamon Press, New York, 1985.
[19] E. Vireton, P. Ganau, J.M. Mackowski, C. Michel, L. Pinard, A. Remillieux, P. Laprat, Nucl. Instrum. Meth. B 95 (1995) 34.
[20] L.R. Doolittle, Nucl. Instrum. Meth. B 15 (1986) 227.
[21] J.P. McCaffrey, B.T. Sullivan, J.W. Fraser, D.L. Callahan, Micron 27 (1996) 407.
[22] S. Reiss, K.-H. Heinig, Nucl. Instrum. Meth. B 112 (1996) 223.
[23] I.M. Lifshitz, V.V. Slyozov, J. Phys. Chem. Solids 19 (1961) 35.
[24] C. Wagner, Z. Elektrochem. 65 (1961) 581.